Numerical study of transverse supersonic flow of monatomic and diatomic gases past a plate

V.A. Titarev*, E.M. Shakhov†, V.A. Rykov** and V. G. Soudakov‡

*University of Trento, Trento, Italy
†Bauman Moscow State Technical University, Moscow, Russia
**Dorodnicyn Computing Center of RAS, Moscow, Russia
‡TsAGI, Zhukovskiy, Russia

Abstract. We investigate supersonic rarefied transverse flow past a cold flat plate in the wide range of Knudsen numbers for both monatomic and diatomic gases on the basis of solving numerically model kinetic equations. For low Knudsen numbers comparison with the Navier-Stokes solution is also provided. We study aerodynamic characteristics of the plate, distribution of the macroparameters over both sides of the plate, temperature anisotropy and appearance of the reverse flow in the bottom vacuum region as functions of Knudsen number, boundary conditions on the plate as well as number of degrees of freedom (monatomic versus diatomic).

Keywords: Shakhov model, Rykov model, supersonic flow, conservative method, implicit TVD scheme
PACS: 47.45.-n

INTRODUCTION

Supersonic flow past a flat thin plate is one of the classical problems of rarefied gas dynamics which is of both academic and practical interest. Most of the published results correspond to the monatomic flow [1, 2, 3, 4, 5, 6, 7, 8]. In particular, in [8] the flow regimes from rarefied to nearly continuum for different boundary conditions were studied. However, the diatomic flow has not been considered in the present literature.

The purpose of the present work is to carry out a comparative study of monatomic and diatomic transverse rarefied flows past a cold plate in the wide range of free-stream Knudsen numbers from the free-molecular to near-continuum flow regimes. The analysis is based on the numerical solutions of the nonlinear model kinetic equations [9, 10, 11] which correctly describe the passage to the continuum regime and are thus well suited for the present study. For small Knudsen numbers we also provide comparison with the compressible Navier-Stokes solution.

For a given free-stream velocity the solution of the problem depends on the number of degrees of freedom (monatomic versus diatomic), Knudsen number, viscosity law and accommodation coefficients in the boundary conditions on the plate surface. We study aerodynamic characteristics of the plate, distribution of the macroparameters over both sides of the plate, temperature anisotropy and appearance of the reverse flow in the bottom vacuum region as functions of these problem parameters.

FORMULATION OF THE PROBLEM

The detailed setup of the problem can be found in [8]. We consider transverse flow of a rarefied gas past a zero-thickness plate of finite width L. The free stream is characterized by the density n_∞, velocity U_∞, temperature T_∞. We introduce a coordinate system with the x axis aligned with the normal to the plate, and y and z axes directed along the plate and spanwise. The plate is assumed to be homogeneous. Then the distribution function does not depend on z.

To save space we describe in detail only the Rykov model equation [11](R-model) used for the kinetic analysis of the diatomic flow. The state of a diatomic gas will be described by the distribution function $f(t,r,\xi,e)$ depending on time t, space $\boldsymbol{r}$, molecular velocity $\boldsymbol{\xi}$ and the energy of rotational movement e. The dimension of the problem can be reduced by passing from f to $\mathbf{g} = (g_1, g_2, g_3)^T$ in the following way:

$$g_1 = \int_{-\infty}^{+\infty}\int_0^\infty f de d\xi_z, \quad g_2 = \int_{-\infty}^{+\infty}\int_0^\infty \xi_z^2 f de d\xi_z, \quad g_3 = \int_{-\infty}^{+\infty}\int_0^\infty e f de d\xi_z$$

Using the same non-dimensional variables as in [8] we write the resulting kinetic equation for $\mathbf{g}$ as follows

$$\frac{\partial \mathbf{g}}{\partial t}+\xi_x\frac{\partial \mathbf{g}}{\partial x}+\xi_y\frac{\partial \mathbf{g}}{\partial y}=\boldsymbol{I},\quad \boldsymbol{I}=\nu_r\mathbf{G}^r+\nu_t\mathbf{G}^t-(\nu_r+\nu_t)\mathbf{g} \tag{1}$$

Here ν_r, ν_t are the frequencies of nonelastic and elastic collisions. The functions $\mathbf{G}_r$, $\mathbf{G}_t$ in the right hand side of (1) have the following form

$$G_1^t=g_M(T_t)\left[1+\frac{8}{15}\frac{(q_x^tv_x+q_y^tv_y)}{p_tT_t}\left(\frac{v_x^2+v_y^2}{T_t}-2\right)\right],\quad G_2^t=\frac{1}{2}T_tg_M(T_t)\left[1+\frac{8}{15}\frac{(q_x^tv_x+q_y^tv_y)}{p_tT_t}\left(\frac{v_x^2+v_y^2}{T_t}-1\right)\right],$$

$$G_3^t=T_r\left[G_1^t+4(1-\delta)g_M(T_t)\frac{(q_x^rv_x+q_y^rv_y)}{p_tT_r}\right],\quad G_1^r=g_M(T)\left[1+\frac{8}{15}\omega_0\frac{(q_x^tv_x+q_y^tv_y)}{pT}\left(\frac{v_x^2+v_y^2}{T}-2\right)\right],$$

$$G_2^r=\frac{1}{2}Tg_M(T)\left[1+\frac{8}{15}\omega_0\frac{(q_x^tv_x+q_y^tv_y)}{pT}\left(\frac{v_x^2+v_y^2}{T}-1\right)\right],\quad G_3^r=T\left[G_1^r+4\omega_1(1-\delta)g_M(T)\frac{(q_x^rv_x+q_y^rv_y)}{pT}\right]$$

where g_M, viscosity and collision frequencies are given by

$$g_M(T)=\frac{n}{\pi T}\exp\left(-\frac{v_x^2+v_y^2}{T}\right),\quad \psi(t)=0.767+0.233t^{-1/6}\exp\left(-1.17(t-1)\right),\quad \mu_t=T_t^{2/3}\frac{\psi(B)}{\psi(BT_t)},$$

$$\nu_t=\frac{8}{5\sqrt{\pi}}\frac{1}{\mathrm{Kn}_\infty}\frac{nT_t}{\mu_t}\left(1-\frac{1}{Z}\right),\quad \nu_r=\frac{8}{5\sqrt{\pi}}\frac{1}{\mathrm{Kn}_\infty}\frac{nT_t}{\mu_t}\frac{1}{Z},\quad B=\frac{T_\infty}{T_*},\quad 1/\delta=1.55$$

Here $\mathrm{Kn}_\infty=\lambda_\infty/L$ is the free-stream Knudsen number, λ_∞ being the mean free path at infinity. The ratio of elastic to non-elastic collisions Z approximates the results of [12] and is given by [13]

$$Z(T_t,T_r)=\frac{3}{4}\pi\frac{\psi(BT_t)}{(BT_t)^{1/6}}\frac{9BT_t}{BT_t+8}\left(\frac{T_r}{T_t}\right)\left[0.461+0.5581\left(\frac{T_r}{T_t}\right)+0.0358\left(\frac{T_r}{T_t}\right)^2\right]$$

We note that the dependence of Z on temperatures is essential; the use of a constant value of Z may lead to wrong results. For nitrogen we have$T_*=91.5^o$ K, $\omega_0=0.2354$, $\omega_1=0.3049$, see [14] . The macroparameters are found as integrals of the distribution function with respect to ξ:

$$\left(n,nu_x,nu_y,\frac{3}{2}nT_t+n(u_x^2+u_y^2)\right)=\int\left(g_1,\xi_xg_1,\xi_yg_1,(\xi_x^2+\xi_y^2)g_1+g_2\right)d\xi_xd\xi_y,\quad nT_r=\int g_3d\xi_xd\xi_y,\quad p_t=nT_t,$$

$$(q_x^t,q_y^t)=\frac{1}{2}\int(v_x,v_y)\left((v_x^2+v_y^2)g_1+g_2\right)d\xi_xd\xi_y,\quad (q_x^r,q_y^r)=\frac{1}{2}\int(v_x,v_y)g_3d\xi_xd\xi_y,\quad \frac{5}{2}T=\frac{3}{2}T_t+T_r,\quad p=nT$$

At infinity upstream of the plate we set the distribution function equal to the locally maxwellian with the free-stream parameters. On the plate we use the boundary condition of the diffusive reflection

$$(g_1,g_2,g_3)_w=\frac{n_w}{\pi T_a^t}\left(1,\ \frac{1}{2}T_a^t,\ T_a^r\right)\exp\left(-(\xi_x^2+\xi_y^2)/T_a^t\right)\quad\text{for}\quad \xi_n>0 \tag{2}$$

where n_w and T_a^t, T_a^r are computed from

$$T_a^t=\frac{E_i^t}{N_i}-(\alpha_t+\alpha_t^r)\left(\frac{E_i^t}{N_i}-T_w\right)+\frac{1}{2}\alpha_r^t\left(2\frac{E_i^r}{N_i}-T_w\right),\quad T_a^r=2\frac{E_i^r}{N_i}-(\alpha_r+\alpha_r^t)\left(2\frac{E_i^r}{N_i}-T_w\right)+2\alpha_t^r\left(\frac{E_i^t}{N_i}-T_w\right)$$

$$E_i^t=-\frac{1}{2}\int\limits_{\xi_n<0}\xi_n\left((\xi_x^2+\xi_y^2)g_1+g_2\right)d\xi_xd\xi_y,\quad E_i^r=-\frac{1}{2}\int\limits_{\xi_n<0}\xi_ng_3d\xi_xd\xi_y\quad N_i=-\int\limits_{\xi_n<0}\xi_ng_1d\xi_xd\xi_y,\quad n_w=2\sqrt{\frac{\pi}{T_a^t}}N_i$$

Here α_t, α_r - are the accommodation coefficients for the translational and rotational degrees of freedom, α_r^t, α_t^r describe the energy transfer from the translational to rotational degrees of freedom and vice versa during the gas

interaction with the plate surface. The values of α_t, α_r, α_t^r, α_r^t are found from the condition that the computed and experimental results agree. Parameters T_a^t, T_a^r are found from the balance conditions of the translational and rotational energy of gas in its interaction with the surface. See [15, 16] for more details.

In the present study two sets of accommodation coefficients in the boundary condition (2) have been used. The first one corresponds to the idealized boundary condition of the complete accommodation and is similar to that used for the monatomic gas:

$$\alpha_t = 1, \quad \alpha_r = 1, \quad \alpha_t^r = 0, \quad \alpha_r^t = 0 \tag{3}$$

In the second set the values of accommodation coefficients have been found from the analysis of experimental data [15, 16]:

$$\alpha_t = 0.8, \quad \alpha_r = 0.5, \quad \alpha_t^r = 0.1, \quad \alpha_r^t = 0.8 \tag{4}$$

For the monatomic gas the Shakhov model kinetic equation (S-model) is used [9, 10]. The details formulation of the problem for this model can be found in [8]. In the monatomic case the boundary condition of complete temperature accommodation of molecules to the surface temperature T_w (cold plate), similar to (3), is used throughout.

RESULTS

The calculations of the flow past the plate were carried out for $0.003 \le \mathrm{Kn} \le \infty$ and the non-dimensional free-stream velocity $U_\infty = 5$. For the monatomic gas we use $\mu = \sqrt{T}$ (hard-sphere law), the Prandtl number $\mathrm{Pr} = 2/3$ and the boundary conditions corresponding to the cold plate ($T_w = T_\infty = 1$). For nitrogen we use $B = 0.3$, corresponding to the free-stream temperature of 27.45^o K.

The problem was solved numerically on a given mesh in variables x, y, ξ_x, ξ_y. For $\mathrm{Kn}_\infty \ge 1$ we use an improved version of steady iteration method. As compared to the conventional method [1], the improvements are twofold: i) we use the second-order advection scheme with discontinuity fitting [5] rather than the first order one, ii) explicit treatment of discontinuities is also used in computing the molecular velocity integrals [6]. The resulting scheme is significantly more accurate in the bottom vacuum region after the plate as compared to both [1, 5]. For low Kn we switch to an implicit second-order accurate time-marching method, conservative with the respect to the collision operator. The method was developed in [8] for S-model equation; extension to the R-model is straightforward and is omitted here. In order to resolve the flow properties better, a non-uniform spatial mesh was used with very small cells near the plate for both large and small Knudsen number computations.

The most tedious are the calculations for low Knudsen numbers. The corresponding computational mesh consisted of 110×140 cells in the spatial variables and 60×30 gridpoints in the variables ξ_x, ξ_y. The total cell number of the four dimensional computational grid was 25 millions. Across the plate, there were 30 mesh cells with grid refinement toward the plate edges. Mesh refinement in the x coordinate, near the plate surface, was so performed that in the Knudsen layer immediately adjacent to the surface the cell size was $\Delta x \approx 10^{-4}$ whereas near the edges $\Delta y \approx 10^{-3}$. The $\mathrm{Kn}_\infty = 0.003$ case required around 10^4 time steps. The computer time required for calculating one iteration per million gridpoints on a personal computer with a clock rate of 3 GHz was 2 to 3 s for the Shakhov model and around 10 s for the Rykov model. The calculation of the results presented below required several months of computer time.

We first study the aerodynamic characteristics of the plate such as the drag c_D and heat transfer c_H coefficients given by the following expressions

$$c_D = \frac{2}{U_\infty^2} \int\limits_{-1/2}^{1/2} (P_{xx}(0-,y) - P_{xx}(0+,y))\, dy, \quad c_H = \frac{1}{E_{x,\infty}} \int\limits_{-1/2}^{1/2} \big(E_x'(0-,y) - E_x(0+,y)\big)\, dy.$$

Here the free-stream energy flux is $E_{x,\infty} = \frac{1}{2}(U_\infty^3 + \frac{5}{2}U_\infty)$ for the monatomic gas and $E_{x,\infty} = \frac{1}{2}(U_\infty^3 + \frac{7}{2}U_\infty)$ for the diatomic gas. Fig. 1 illustrates the dependence of c_D and c_H on Kn for both kinetic and Navier-Stokes solutions. For the latter the Sutherland viscosity model is used in the diatomic case whereas in the monatomic case we take $\mu = \sqrt{T}$ as in the S-model equation. Even for the equivalent boundary condition (3) the monatomic and diatomic results differ in the entire range of Knudsen numbers, see left and center pictures. The Navier-Stokes solution for the drag coefficient agrees reasonably well with the kinetic one only for sufficiently small values of Kn. However, the heat transfer coefficient obtained by the continuums solution is quite different from the kinetic one, the difference is about 30% in the monatomic case and around 10% in the diatomic one. The influence of the accommodation coefficients in

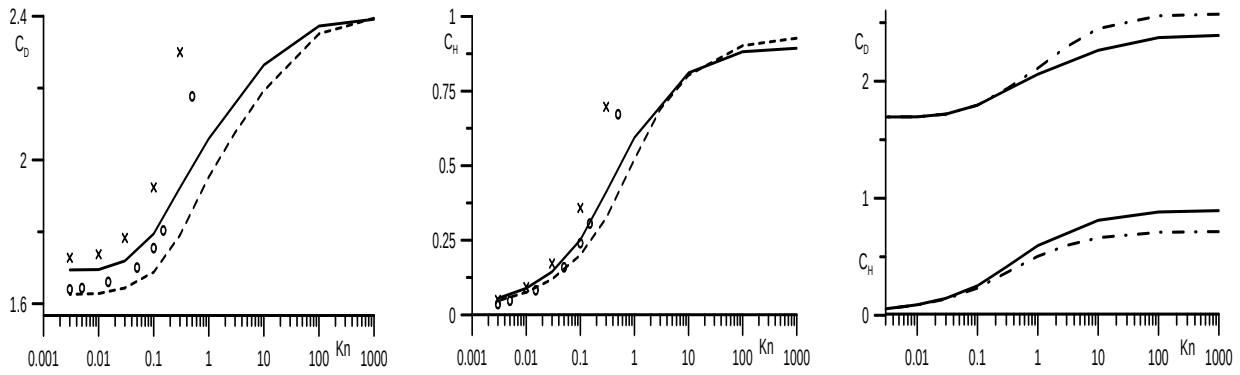

FIGURE 1. Aerodynamic characteristics of the plate. Solid line - nitrogen for b.c. (3), dashed line - monatomic solution, dashed-dotten line - nitrogen for b.c. (4), circles - monatomic Navier-Stokes solution, crosses - diatomic Navier-Stokes solution.

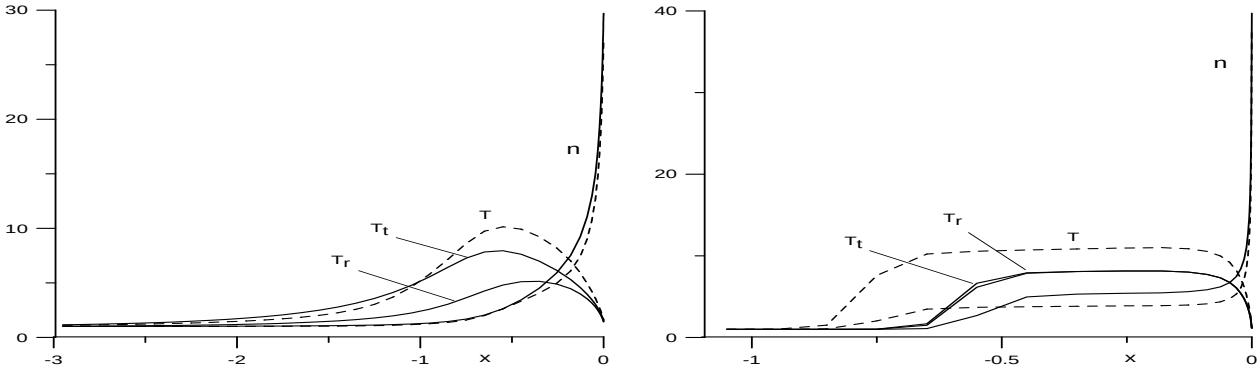

FIGURE 2. Density and temperature distribution on the symmetry line for $\mathrm{Kn}_\infty = 0.3$ (left) and $\mathrm{Kn}_\infty = 0.003$ (right). Solid line - nitrogen for b.c. (3), dashed line - monatomic kinetic solution, dashed-dotted line - monatomic Navier-Stokes solution.

the diatomic case is very pronounced for large and transitional Knudsen numbers but decreases as $\mathrm{Kn}_\infty \to 0$, see the right picture of Fig. 1.

The overall flow pattern for nitrogen is similar to the monatomic case studied in detail in [8] and is omitted here. The influence of the degrees of freedom is mostly seen in distribution of macroparameters on the symmetry line in front of the plate as well as over the plate. Fig. 2 depicts profiles of density, translational and rotational temperatures for Knudsen numbers $\mathrm{Kn}_\infty = 0.3$ (left) and $\mathrm{Kn}_\infty = 0.003$ (right). We see a standard flow pattern with a forming bow shock wave and a thin boundary layer near the plate. It is interesting to note that the profiles of density and temperature are shifted with respect to each other in the shock wave profile. For $\mathrm{Kn}_\infty = 0.003$ the Navier-Stokes profiles agree reasonably well with the kinetic solution.

Fig. 3 depicts distributions of density, normal stress and normalized energy flux over the downwind side of the plate for $\mathrm{Kn}_\infty = 0.3$. It is obvious, that the monatomic and diatomic results differ very significantly. Also the influence of the accommodation coefficients is rather large. As the Knudsen number decreases, the differences become smaller although still visible. The corresponding plots are omitted. We note that gas density on the upwind side of the plate is larger for nitrogen for all Knudsen number. However, it does not automatically result in large density values on the downwind side.

Fig. 4 shows comparisons of the kinetic and Navier-Stokes solutions for density, normal stress and normalized energy flux on the downwind side of the plate for $\mathrm{Kn}_\infty = 0.003$ and diatomic gas with b.c. (3). Significant differences are observed even for this rather small Knudsen numbers. We note that the Navier-Stokes solution has an nonphysical singularity near the edge of the plate. On the upwind side of the plate the normal stress distributions virtually coincide.

Fig. 5 shows contour lines of translational and rotational temperatures of nitrogen for $\mathrm{Kn}_\infty = 0.3$ and $\mathrm{Kn}_\infty = 0.003$ for the b.c. 3. We see that for $\mathrm{Kn}_\infty = 0.3$ the distribution of T_t and T_r are quite different especially near the plate. This means that the flow is far from the equilibrium. For the second, much smaller Knudsen number both temperatures virtually coincide except a small zone in the bottom vacuum region after the plate.

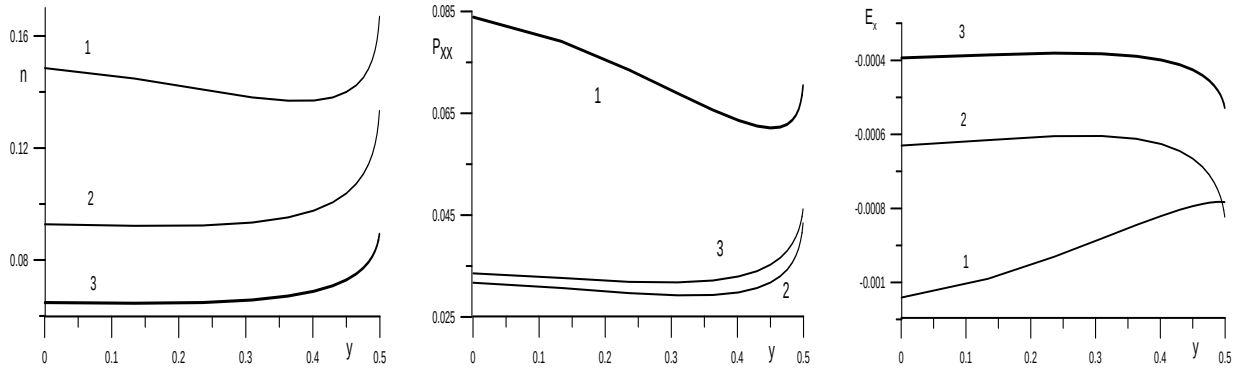

FIGURE 3. Density, normal stress and energy flux distribution over the downwind side of the plate for $Kn_\infty = 0.3$; 1 – monatomic gas, 2,3 - nitrogen for b.c. (3),(4), respectively.

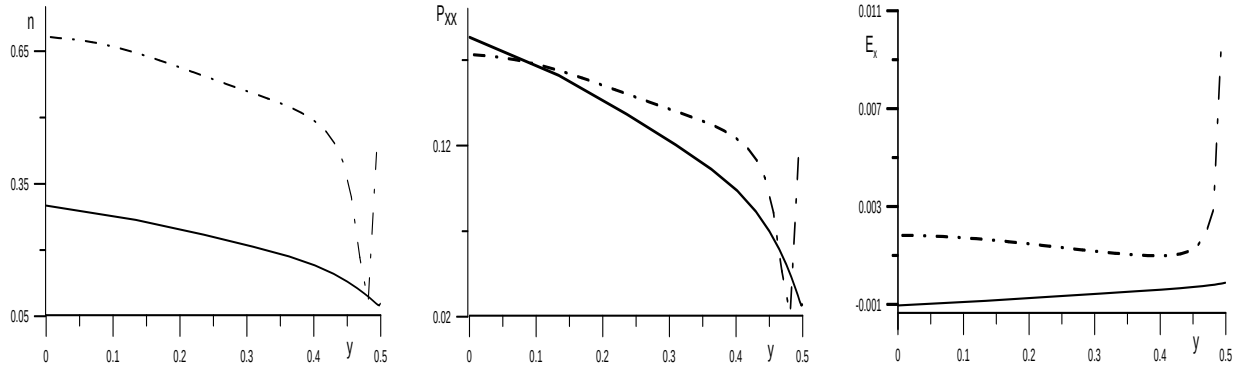

FIGURE 4. Kinetic (solid line) versus Navier-Stokes (dashed-dotted line) solutions for $Kn_\infty = 0.003$, diatomic gas and the downwind part of the plate.

Finally, Fig. 6 shows flow streamlines for nitrogen. We observe the formation of the circulation zone after the plate for sufficiently small Knudsen numbers.

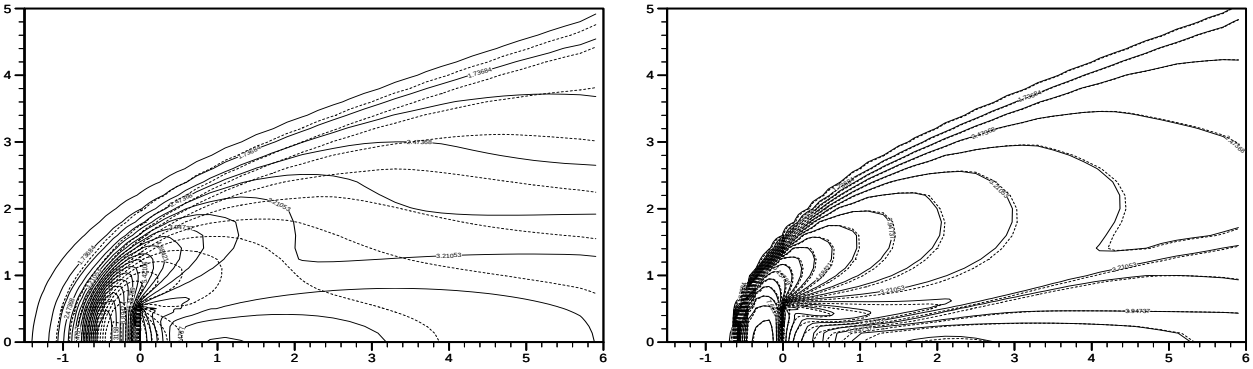

FIGURE 5. Translational (solid line) and rotational (dashed line) temperature distributions in nitrogen for $Kn_\infty = 0.1$ (left) and $Kn_\infty = 0.003$ (right); b.c. (3) is used. 20 contour levels from 1 to 8.

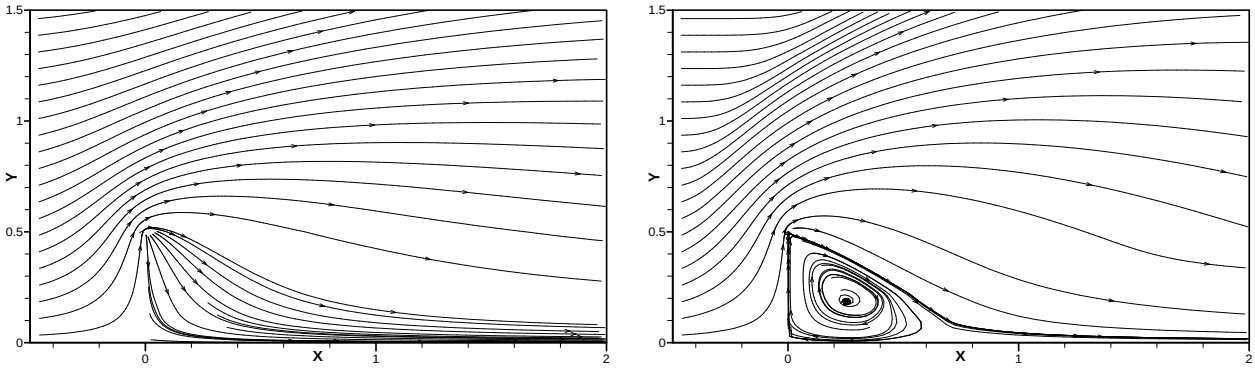

FIGURE 6. Streamlines in nitrogen for $\mathrm{Kn}_\infty = 0.1$ (left) and $\mathrm{Kn}_\infty = 0.003$ (right); b.c. (3) is used.

CONCLUSIONS

We have studied supersonic monatomic and diatomic transverse flow of rarefied gas over a cold flat plate in the wide range of Knudsen numbers and provided comparison with the Navier-Stokes solution. The presented results show significant differences between monatomic and diatomic gases as well as the Navier-Stokes solution. Additionally, accommodation coefficients in the boundary conditions on the plate have a visible influence on results for large and transitional Knudsen numbers.

ACKNOWLEDGMENTS

The first author acknowledges the financial support provided by the PRIN programme (2004-2006) of Italian Ministry of Education and Research (MIUR). He would also like to thank Professor E.F. Toro OBE for numerous discussions on the construction of the Godunov-type methods. The second and third authors acknowledge the partial support of the Russian Foundation for Basic Research (project No. 04- 01-00347).

REFERENCES

1. E. M. Shakhov, *Fluid Dynamics* **7**, 961 – 966 (1972).
2. E. M. Shakhov, *Fluid Dynamics* **8**, 275 – 281 (1973).
3. A. I. Erofeev, and V. A. Perepuhov, *Fluid Dynamics* **11**, 579–585 (1976).
4. E. M. Shakhov, "Numerical studies on rarefied gas flow over a flat plate at an angle of attack," in *Proceedings of 15th Intern. Symp. on Rarefied Gas Dynamics, V.I.*, B.G.Teubner Stuttgart, 1986, pp. 482–491.
5. K. Aoki, K. Kanba, and S. Takata, *Phys. Fluids* **9**, 1144–1161 (1997).
6. V. A. Titarev, and E. M. Shakhov, *J. Comp. Math. Math. Phys.* **41**, 1372–1384 (2001).
7. R. V. Maltsev, and A. K. Rebrov, *Fluid Dynamics* **40**, 140–147 (2005).
8. V. A. Titarev, and E. M. Shakhov, *Fluid Dynamics* **40**, 790–804 (2005).
9. E. M. Shakhov, *Fluid Dynamics* **3**, 156–161 (1968).
10. E. M. Shakhov, *Fluid Dynamics* **3**, 142–145 (1968).
11. V. A. Rykov, *Fluid Dynamics* **10**, 959–966 (1975).
12. J. Lordi, and R. Mates, *Phys. Fluids* **13**, 291–308 (1970).
13. I. N. Larina, and V. A. Rykov, *Dokl. Akad. Nauk. USSR* **227**, 60–62 (1976).
14. I. N. Larina, and V. A. Rykov, "Hypersonic flows of a rarefied gas past conical bodies," in *Soobsheniya po prikladnoy matematike*, Dorodnicyn Computing Center of Soviet Academy of Sciences, 1990.
15. I. N. Larina, and V. A. Rykov, *Fluid Dynamics* **21**, 795 – 801 (1986).
16. I. N. Larina, and V. A. Rykov, "The boundary condition on the body surface for a diatomic gas," in *Rarefied Gas Dynamics. Proc. 15th Int. Symp.*, edited by V. Boffi, and C. Cercignani, B.G. Teubner Stuttgart, 1986, vol. 1, pp. 635–643.